A&A 373, 905–915 (2001)
DOI: 10.1051/0004-6361:20010672

Astronomy & Astrophysics

VLT observations of turnoff stars in the globular cluster NGC 6397⋆

F. Thévenin[1], C. Charbonnel[2], J. A. de Freitas Pacheco[1], T. P. Idiart[3], G. Jasniewicz[4], P. de Laverny[1], and B. Plez[4]

[1] Observatoire de la Côte d'Azur, BP 4229, 06304 Nice Cedex 4, France
[2] Laboratoire d'Astrophysique de Toulouse, CNRS UMR 5572, 14 avenue Édouard Belin, 31400 Toulouse, France
[3] Instituto Astronômico e Geofísico – Av. Miguel Stefano 4200, 04301-904 São Paulo, Brazil
[4] UMR 5024, Université Montpellier II, CC 72, 34095 Montpellier Cedex 5, France

Received 17 January 2001 / Accepted 3 May 2001

Abstract. VLT-UVES high resolution spectra of seven turnoff stars in the metal-poor globular cluster NGC 6397 have been obtained. Atmospheric parameters and abundances of several elements (Li, Na, Mg, Ca, Sc, Ti, Cr, Fe, Ni, Zn and Ba) were derived. The mean iron abundance is [Fe/H] = −2.02, with no star-to-star variation. The mean abundances of the alpha-elements (Ca, Ti) and of the iron-peak elements (Sc, Cr, Ni) are consistent with abundances derived for field stars of similar metallicity. Magnesium is also almost solar, consistent with the values found by Idiart & Thévenin (2000) when non-LTE effects (NLTE hereafter) are taken into account. The sodium abundance derived for five stars is essentially solar, but one object (A447) is clearly Na deficient. These results are compatible with the expected abundance range estimated from the stochastic evolutionary halo model of Argast et al. (2000), in which at the epoch of [Fe/H] ∼−2 the interstellar medium is supposed to become well-mixed.

Key words. stars: abundances – Galaxy: globular clusters: individual: NGC 6397 – Galaxy: abundances

1. Introduction

Stars in globular clusters were traditionally considered to be coeval and mono-metallic. However, spectroscopic abundance determinations performed in the past several years indicate intra-cluster variations of several elements in giant stars for all the studied clusters (see Kraft 1994; Da Costa 1998; Sneden 1999 for reviews). The most striking, dominant and common abundance variations concern the light elements involved in the CNO, NeNa and MgAl proton-capture chains, i.e. the CNO, Na, Mg and Al isotopes, as well as Li. The nucleosynthesis responsible for the observed abundance patterns of these elements is very well understood, but the site where this nucleosynthesis occurs is still a matter of debate: did the observed stars pollute their own atmosphere (the so-called "evolutionary", or "deep mixing" scenario), or did they inherit their peculiar composition at their formation (the so-called "primordial" scenario)? In the later case, were the inhomogeneities already present in the interstellar medium from which the cluster formed, or did an early generation of relatively massive, rapidly evolving stars pollute the intra-cluster gas?

In clusters with abundances derived for a large number of giants, some abundance patterns appear which are not seen among their field counterparts. In particular, sodium and oxygen are clearly anti-correlated. This behaviour was demonstrated to be present in M 3 (Kraft et al. 1992), M 5 (Sneden et al. 1992), ω Cen (Paltoglou & Norris 1989; Norris & da Costa 1995), M 13 (Peterson 1980; Kraft et al. 1993; 1997), M 15 (Sneden et al. 1997), NGC 7006 (Kraft et al. 1998), M 4 (Ivans et al. 1999), M 92 (Shetrone 1996a) and M 10 (Kraft et al. 1995), over a wide range of metallicity ($-2.5 \leq$ [Fe/H] ≤ -1). It can easily be understood from a nucleosynthesis point of view: ^{23}Na production via proton capture reactions (NeNa cycle) becomes active at the same temperature as the ON branch of the CNO bicycle ($T \sim 3 \times 10^7$ K), which is reached in the hydrogen burning shell of low mass RGB stars (Denissenkov & Denissenkova 1990; Langer et al. 1993). Thus Na-O anticorrelation can in principle be explained in the framework of a deep-mixing scenario along the RGB, while it requires a deeper mixing than the C and N anomalies do (Denissenkov & Weiss 1996; Cavallo et al. 1998; Palacios et al. 1999; Weiss et al. 2000).

Aluminium and sodium abundances have been determined only for a few clusters and the available data show a clear correlation between these elements (Shetrone 1996b; Kraft et al. 1997, 1998; Ivans et al. 1999), which are both anti-correlated with magnesium (Norris & Da Costa 1995;

Send offprint requests to: F. Thévenin,
e-mail: thevenin@obs-nice.fr

⋆ Based on data collected at Paranal Observatory (ESO, Chile)-Proposal:65.L-0654(A).

Zucker et al. 1996; Pilachowski et al. 1996; Sneden et al. 1997; Ivans et al. 1999). While the proton capture reaction ^{22}Ne(p,γ)^{23}Na can explain the sodium production in low mass RGB stars, the reaction ^{24}Mg(p,γ)^{25}Al requires a temperature largely above that reached by the hydrogen-burning shell (70–85 MK, where the maximum temperature reached in canonical models is only of ∼55 MK). According to Ivans et al. (1999), the Al-Mg variations in M 4 could be explained if aluminium is produced at the expense of the isotopes ^{25}Mg and ^{26}Mg, but this requires a significant enhancement of the initial abundances of these isotopes (Denissenkov et al. 1998).

However, so far, all these abundance variations have been observed only in evolved stars close to the RGB tip (except in M 13 for which very sparse data exist for some stars next to the RGB bump). Nevertheless, in 47 Tuc, and in NGC 6752 CN and Na variations are already detected in turnoff stars (Cottrell & Da Costa 1981; Briley et al. 1994, 1995), opening the possibility that primordial or external pollution mechanisms could also have affected the original chemical pattern (see also Denissenkov et al. 1998). More recently, from high resolution spectroscopy obtained with the 10 m Keck I telescope, King et al. (1998) derived LTE abundances for seven subgiant stars in the metal-poor cluster M 92. They concluded that the abundance ratios [Cr/Fe], [Ca/Fe] and [Ti/Fe] are the same as those observed in the field stars, but remarkable differences exist for the ratios [Mg/Fe] and [Na/Fe]. From the theoretical point of view, it is difficult to interpret these results in the framework of the deep-mixing scenario, for at least three reasons. First, because the onset of this mechanism is supposed to occur only after the star reaches the RGB bump (e.g. Charbonnel et al. 1998 and references therein). Second, because the temperature required to activate the NeNa chain is not attained before the star reaches the RGB. Last but not least, there is no evidence for lithium depletion in any subgiants.

Observations of less evolved stars down to the turnoff of globular cluster are badly needed in order to disentangle the primordial and deep-mixing scenarios. Here we report high-resolution spectroscopy performed with the VLT of seven turnoff stars in the globular cluster NGC 6397. This cluster was chosen because of its relative small distance (∼2.2 kpc), which permits the study of turnoff stars with a reasonable signal-to noise ratio. Castilho et al. (2000) have recently reported abundances for five giants and eleven subgiants in this cluster, which are complementary to our own investigation. The plan of this paper is the following: in Sect. 2 the observations are described as well as the derivation of the stellar parameters; in Sect. 3 the stellar abundances are obtained and results are discussed. Finally, in Sect. 4 the concluding remarks are given.

2. Observations and stellar parameters

The program stars were taken from an extensive list of cluster members prepared by Alcaino et al. (1997) and selected, according to their colors, by their location in the turnoff region of the HR diagram. The program stars and their basic photometric data are given in Table 1. Identification numbers are the same as in Alcaino et al. (1997). The spectra were obtained with the UVES spectrograph (Dekker et al. 2000) attached to the second VLT unit (Kueyen telescope), during June and July 2000. A total of 28 spectra of one hour exposure each were taken, corresponding to four spectra per object. The wavelength range covered by our spectra is 4780–5755 Å and 5835-6800 Å and the slit width was about 1.1″, corresponding to a spectral resolution of ≈40 000. The mean seeing during the observations was ∼1″. In order to estimate the S/N ratio of our data, the average and the standard deviation of the relative flux were calculated using bins of 500 pixels, corresponding to 17 Å and 15 Å for spectra obtained with the red and the blue spectrograph arms, respectively. The S/N ratio varies from 75 in the blue up to 95 in the red.

The magnitude range and the $(B-V)$ colors of the program stars are quite narrow because we wanted to have similar atmospheric parameters, preventing differences in the stellar chemical abundances from being due to their evolutionary stage.

The UVES Data Reduction Standard Pipeline (Ballester et al. 2000) was used for the reduction of the spectra. Then a detailed data treatment was performed using MIDAS and IRAF facilities. For each star and given spectral range, the four images were first averaged and the resulting spectrum was binned by two pixels as well as corrected to the local standard of rest. At this step, each pixel corresponds to 0.0294 Å in the blue and 0.0348 Å in the red. Finally, each image was normalized with respect to the stellar continuum. Radial velocities derived from our data are given in Table 1. The mean value is $16.7 \pm 4.0\,\mathrm{km\,s^{-1}}$, consistent with the mean radial velocity of $18.9\,\mathrm{km\,s^{-1}}$ given by Harris (1996).

The spectral lines selected for abundance determination purposes are, in general, those with accurate $\log gf$ and not blended. Equivalent widths of 55 lines satisfying our criteria were measured using a Gaussian fitting procedure, and are given in Table 2. Errors in equivalent widths were estimated by using Cayrel's (1987) relation and are typically of the order of 1.4 mÅ. If errors in positioning of the continuum are also taken into account, then the expected mean error of our equivalent widths is about 2.8 mÅ.

2.1. Effective temperatures

In order to obtain precise photospheric abundances, the effective stellar temperature $T_{\rm eff}$ and the surface gravity g need to be estimated quite accurately.

The reddening in the direction of NGC 6397 was first estimated by Eggen (1960), who derived a color excess $E(B-V) = 0.15$. More recent estimates are those by Djorgovski (1993) and Alcaino et al. (1997), who obtained respectively $E(B-V) = 0.18$ and 0.17. The reddening

Table 1. Program stars. Photometric data are from Alcaino et al. (1997). Column 7 corresponds to $T_{\rm eff}$ in the scale of Alonso et al. (1996) adopting $E(B-V) = 0.18$. The final adopted temperature (Col. 10) is defined in the text.

Ident (1)	V (2)	S/N(mean) (3)	$(B-V)$ (4)	$(V-I)$ (5)	$V_{\rm R}$(km s^{-1}) (6)	$T_{\rm eff}(B-V)$ (7)(K)	$T_{\rm eff}(\rm H_\alpha)$ (8)(K)	$T_{\rm eff}(\rm H_\beta)$ (9)(K)	$T_{\rm eff}$(adop) (10)(K)
A228	16.068	90	0.567	0.827	14.6	6199	6172	6185	6185
A447	16.185	80	0.584	0.801	16.7	6125	6190	6161	6159
A575	16.167	75	0.573	0.813	18.1	6173	6172	6172	6172
A721	16.203	75	0.549	0.813	15.9	6279	6280	6280	6280
A1406	16.145	75	0.560	0.827	10.1	6230	6285	6285	6265
A2084	16.198	70	0.542	0.830	16.7	6310	6335	6335	6330
A2111	16.011	95	0.598	0.867	24.6	6066	6080	6075	6075

value is an important correction to the photometric data if these are used to derive the effective temperature. We adopt in the following $E(B-V) = 0.18$, and as an exercise to check this value we explored the possibility to use the NaD interstellar lines. From a de-blending procedure, we obtained $W(\lambda5889) = 0.301 \pm 0.065$ Å and $W(\lambda5896) = 0.232 \pm 0.050$ Å for the interstellar components. Using the doublet ratio method, we found a column density $N(\rm Na) = 2.3 \times 10^{12}$ cm^{-2}. The statistical correlation between the color excess and the interstellar sodium column density derived from data by Cohen (1975) is

$$E(B-V) = -6.89 + 0.571 \log N(\rm Na) \quad (1)$$

from which we get $E(B-V) = 0.17$. This result is consistent with previous independent estimates.

We adopted two different procedures to estimate effective temperatures. First, temperatures were computed from $(B-V)_0$ colors, using the calibration by Alonso et al. (1996) for low main sequence stars, with spectral types ranging from F0 to K5 and metallicities in the interval $-2.5 \leq$ [Fe/H] ≤ 0. This temperature scale was established from infrared photometry and scaled directly to $T_{\rm eff}$ determinations via reliable angular diameter measurements. This color-temperature relationship is in good agreement with that derived recently by Sekiguchi & Fukugita (2000) for the same spectral range and metallicities [Fe/H] ≤ -1.5. The standard deviation of the relation $(B-V)_0$ vs. $T_{\rm eff}$ is about 130 K, depending slightly on the metallicity. According to Alonso et al. (1996), the mean variation $\Delta T_{\rm eff}/\Delta(B-V)$ is about 30 K per 0.01 mag and if we take into account: *i)* a typical random photometric error of 0.01 mag in B and V and *ii)* a typical error of 0.04 mag in the reddening (Alcaino et al. 1997), the expected error in $T_{\rm eff}$ is ±140 K.

A second independent estimate of the effective temperature can be obtained from Hα and Hβ line profiles, since wings are very sensitive to this parameter. We have fitted our profiles to theoretical ones computed with the atmospheric models by Gustafsson et al. (1975), taking into account self-resonance broadening according to the prescriptions by Cayrel & Traving (1960), and Stark broadening of the wings (Vidal et al. 1973; Stehlé et al. 1983). The code used in our computations is from F. Praderie & A. Talavera (private communication). From our fits, temperatures can be estimated within errors of about 40 K. In spite of the difficulty in obtaining good flat-field corrections on echelle spectra, the use of both Hα and Hβ lines reduces errors induced by that procedure, an error of 80 K will probably be more realistic. More accurate determinations require knowledge of the surface gravity and metallicity.

We therefore used an iterative procedure as well as NLTE gravities and metallicities derived according to the method by Thévenin & Idiart (1999). We have verified that, using our procedure and Balmer line profiles, errors of the order of 0.1 dex in log g induce errors of about 40 K in the temperature. A variation of 0.2 dex in the

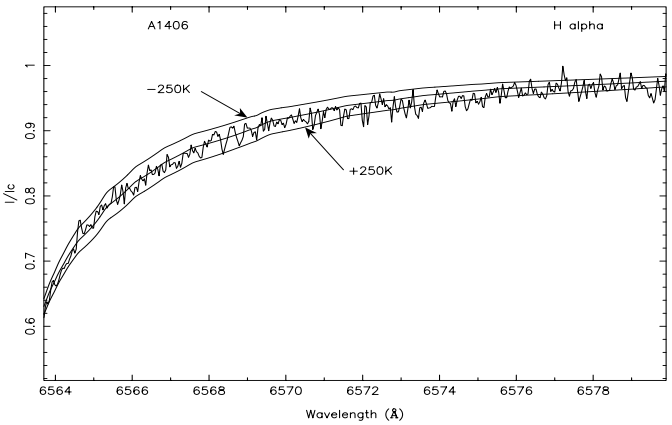

Fig. 1. Fit of Hα line profile of the star A1406.

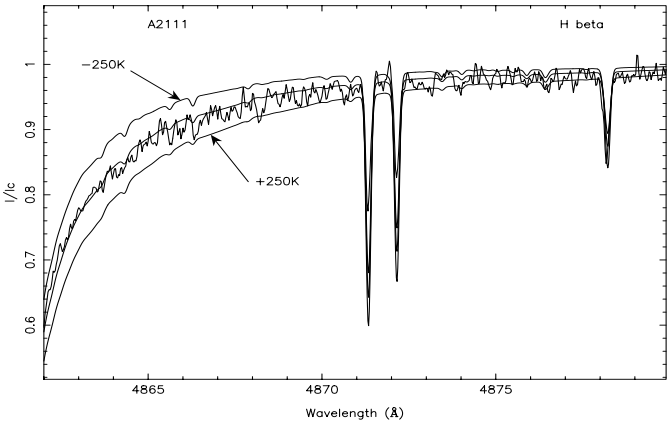

Fig. 2. Fit of Hβ line profile of the star A2111.

Table 2. Measured equivalent widths (mÅ) and adopted line parameters. a: Thévenin (1989, 1990), b: Wiese et al. (1969, 1980), c: Warner (1968), d: Miles et al. (1969), e: Martin et al. (1988), f: Smith et al. (1981), g: Castilho et al. (2000).

Ident	λ(Å)	EP(eV)	log gf	228	447	575	721	1406	2084	2111
Zn1	4810.537	4.08	−0.14 c	9.1	8.7	9.2	7.8	0.0	10.1	6.0
Fe1	4890.763	2.87	−0.47 a	32.8	30.5	31.7	30.3	33.9	31.8	35.3
Fe1	4891.502	2.85	−0.17 a	47.7	41.8	42.4	44.0	43.8	43.5	49.5
Cr2	4824.143	3.87	−0.94 a	8.1	6.8	5.3	5.0			7.5
Fe1	4903.316	2.88	−1.10 a	12.8	12.0	12.6	10.7			16.2
Fe1	4918.998	2.86	−0.41 a	33.5	33.1	34.8	29.3	34.0	31.7	39.0
Fe1	4920.514	2.83	0.04 a	55.9	53.5	55.3	49.6	51.9	54.3	59.7
Fe2	4923.930	2.89	−1.43 a	60.9	60.1	58.2	57.3	55.4	60.6	61.4
Ba2	4934.095	0.00	−0.16 d	36.3	29.2	32.6	28.4	25.6	30.2	40.5
Fe1	4966.094	3.33	−0.73 a	9.9	8.0	10.3	8.0		9.9	
Ti1	4981.740	0.85	0.52 a	17.5	25.3	18.2	17.5	18.1	18.6	23.9
Ti1	4991.072	0.84	0.41 a	20.0	20.6	14.6	15.7	16.8	19.5	19.8
Ti1	4999.510	0.83	0.25 e	14.4	16.0	14.9	9.4	11.4	14.7	18.2
Fe1	5001.870	3.88	−0.25 a	12.5	10.9	10.2	9.5	9.3	10.7	13.2
Fe1	5014.951	3.94	−0.28 a	12.5	8.2	10.2	9.7		8.5	8.8
Fe2	5018.446	2.89	−1.24 a	72.4	68.3	68.9	68.4	71.4	67.2	72.5
Fe1	5049.827	2.28	−1.46 a	15.9	13.1	17.6	16.0	14.9	14.9	21.3
Ti2	5129.162	1.89	−1.39 e	11.6	11.8	9.2	7.9	9.2	12.2	11.3
Fe1	5133.699	4.18	0.14 a	15.5	15.6	15.8	15.1	13.1	10.9	14.6
Fe1	5162.281	4.18	0.09 a	13.5	13.5	11.7	10.7	13.9	10.8	15.2
Mg1	5172.698	2.71	−0.32 a	147.3	135.3	123.3	124.0	136.5	137.9	140.9
Mg1	5183.619	2.72	−0.08 a	171.2	152.8	143.7	144.8	159.9	153.0	158.8
Ti2	5185.908	1.89	−1.35 e		14.5	12.4	8.7	8.5	11.3	13.8
Fe1	5192.353	3.00	−0.50 a	25.9	27.8	29.7	28.9	25.0	21.7	29.1
Fe1	5194.949	1.56	−2.15 a	16.2	12.2	15.2	13.3	15.4	16.4	19.7
Cr1	5206.044	0.94	0.03 a	34.8	32.7	35.5	29.9	33.4	32.4	39.0
Fe1	5216.283	1.61	−2.17 a	12.7	12.1	12.8	10.5	11.3	11.1	17.7
Fe2	5234.630	3.22	−2.31 a	13.5	10.8	12.4	9.9	10.9		14.2
Fe1	5269.550	0.86	−1.42 a	83.0	81.4	81.3	81.2	84.1	84.2	89.4
Fe2	5316.620	3.15	−1.89 a	30.7	27.2	32.1	29.0	28.5	29.7	30.3
Ti2	5336.794	1.58	−1.70 e	10.2		9.2	7.2	9.8		
Ca1	5349.469	2.71	−0.31 f	8.0	7.9	8.4	8.3		8.8	8.2
Fe1	5364.880	4.44	0.20 a	8.9	8.0	8.7	8.5	9.2		11.7
Fe1	5367.476	4.41	0.26 a	10.0	11.5	10.1	11.6		10.2	12.9
Fe1	5383.380	4.31	0.48 a	21.0	18.0	21.6	20.3	15.6	20.5	19.4
Fe1	5405.785	0.99	−1.98 a	54.4	51.5	51.5	49.8	49.5	47.4	60.2
Fe1	5415.210	4.39	0.51 a	18.3		18.0	15.9	17.7	15.7	18.8
Fe1	5424.080	4.32	0.55 a	22.8	22.5	24.5	23.1	23.9	19.6	24.5
Fe1	5434.534	1.01	−2.22 a	37.8	37.9	41.6	33.9	37.1	36.2	46.0
Ni1	5476.921	1.83	−0.89 e	20.8	14.6	19.5	16.8	15.5	13.4	27.1
Fe1	5497.526	1.01	−2.75 a	14.3	12.0	15.8	13.3	13.9	11.6	16.3
Fe1	5506.791	0.99	−2.85 a	15.0	10.8	10.6	10.6	10.6	9.9	17.7
Sc2	5526.821	1.77	0.18 a	10.8	10.5	11.4	9.5	11.1	12.5	10.6
Mg1	5528.418	4.34	−0.47 a	40.7	39.0	35.0	31.8	38.1	38.3	40.3
Ca1	5588.764	2.52	0.21 b	29.5	30.2	27.8	28.1	26.8	26.5	32.8
Ca1	5601.286	2.52	−0.52 b	7.7		7.8	8.0		7.3	6.8
Na1	5688.217	2.10	−0.42 g	6.8		7.1				8.0
Ca1	5857.459	2.93	0.24 b	17.8	15.8	17.2	16.2	18.3	18.0	19.1
Ba2	6141.727	0.70	−0.08 d	13.4	11.0	12.7	10.9	11.2	12.3	16.9
Ca1	6162.180	1.90	−0.10 a	45.0	41.4	43.5	37.9	39.6	41.0	46.4
Fe1	6230.736	2.56	−1.24 a	17.7	13.6	15.9	11.0	13.6	12.7	17.3
Fe1	6393.612	2.43	−1.57 a	12.3	12.9	13.6	12.1		11.4	13.8
Ca1	6439.083	2.52	0.39 a	39.3	37.5	37.0	37.7	34.1	36.1	42.9
Fe1	6494.994	2.40	−1.24 a	23.5	18.1	20.8	16.7	15.8	18.1	21.8
Ca1	6717.687	2.71	−0.39 a	8.3	8.7	8.0	8.4			7.9

Table 3. Atmospheric parameters. $\log g_{\rm evol}$ was calculated for a distance of 2.2 kpc. The $T_{\rm eff}$(adopted) corresponds to the mean value of the three determinations reported in Table 1.

Ident	$T_{\rm eff}$(adop)	$\zeta_{\rm turb}$(km s^{-1})	log $g_{\rm LTE}$	log $g_{\rm NLTE}$	log $g_{\rm evol}$	[Fe/H]$_{\rm LTE}$	[Fe/H]$_{\rm NLTE}$
A228	6185	1.30	3.75	4.15	4.05	−2.25	−2.05
A447	6159	1.35	3.75	4.15	4.09	−2.27	−2.05
A575	6172	1.10	3.75	4.15	4.09	−2.24	−2.03
A721	6280	1.20	3.85	4.20	4.13	−2.23	−2.03
A1406	6265	1.20	3.85	4.20	4.11	−2.25	−2.04
A2084	6330	1.30	3.90	4.25	4.15	−2.23	−2.03
A2111	6075	1.15	3.65	4.05	4.00	−2.24	−2.01

metallicity does not affect noticeably the resulting temperature. In order to illustrate our results, the best fit for two stars included in our sample, as well as the resulting profiles if the temperature is altered by ±250 K are shown in Figs. 1 and 2. Temperatures resulting from photometry and fitting of Balmer lines are given in Table 1, as well as the final adopted values (Col. 10), corresponding to the mean of Cols. 7–9. Inspection of these results indicate that temperatures derived from both scales are in quite good agreement and that no systematic effects are observed.

2.2. LTE Surface gravities using LTE iron abundances

The surface gravity is a quantity especially difficult to derive because only few ionized species have measurable lines in the spectra. Moreover, in metal-poor dwarfs, reaching ionization balance is difficult and produces NLTE-overionization (see Magain 1988; Axer et al. 1995; Thévenin & Idiart 1999). In a first approximation, adopting LTE, the surface gravity was estimated by enforcing the equality of abundances derived from FeI and FeII lines, using the curve of growth technique. The microturbulent velocity $\zeta_{\rm turb}$ was derived from the plateau of the curve of growth of FeI. The uncertainties in log g are due to the fit quality of the curve of growth for both FeI and FeII, errors in the oscillator strengths and errors in the equivalent widths. We expect that total errors in LTE gravities are not larger than 0.2 dex.

2.3. NLTE corrections to surface gravities

Inspection of Table 3 indicates that surface gravities of our program stars derived under the assumption of LTE correspond to values expected for subgiant stars (log $g_{\rm LTE} \sim$ 3.7), which are incompatible with the actual position of these objects in the HR diagram. These low derived gravities are caused by overionization effects in FeI and they should be corrected according to the procedure by Thévenin & Idiart (1999) and Idiart & Thévenin (2000). The strengthening of the UV radiation field produced by a reduced opacity in metal-poor stars is the main cause of the overionization effect. Corrected gravities are given in Col. 5 of Table 3. NLTE surface gravities can be checked by comparison with those derived from the expected value, according to the position of the star in the HR diagram, given by the relation

$$\log g_{\rm evol} = -10.537 + \log (M/M_\odot) + 4 \log T_{\rm eff} + 0.4(V_0 + BC) - 2 \log d \qquad (2)$$

where M is the stellar mass, BC is the bolometric correction, d is the distance in parsecs and the solar quantities log $g_\odot = 4.44$, $T_\odot = 5772$ K and $M_{\rm bol}(\odot) = 4.75$ were adopted to obtain the numerical constant. Assuming $M = 0.85\ M_\odot$ as a typical value for a cluster turnoff star and $d = 2200$ pc (Djorgovski 1993), the evolutionary gravities can be estimated using photometric data and our derived temperatures. These gravities are also given in Table 3 (Col. 6) and are entirely consistent with our NLTE values.

3. The chemical abundances

3.1. LTE abundances

LTE abundances were derived by adopting effective temperatures and gravities given in Table 3 and by using the stellar atmosphere models of Gustafsson et al. (1975) and recent models issued from the MARCS code (Plez et al. 1992; Asplund et al. 1997; Edvardsson et al. 1993). The resulting abundances with respect to the solar value (Holweger 1979) and references for the adopted log gf are given in Table 4. For the elements Na, Zn, Sc and Ni there was only one faint measurable line and thus the abundance determination for these elements is more uncertain when compared to others. Typical errors in $T_{\rm eff}$, log g, [Fe/H] and $\zeta_{\rm turb}$ are respectively equal to 80 K, 0.1 dex, 0.1 dex and 0.2 km s^{-1}, corresponding to abundance errors of about 0.1 dex, which is adopted here as the error in our final abundance values.

3.2. LTE abundances deduced using log $g_{\rm NLTE}$

We have also computed LTE abundances using model atmospheres adopting the corrected NLTE iron abundances and surface gravities (see Table 5), for two main reasons. First, because the Li abundance is practically unaffected by NLTE effects (Carlsson et al. 1994). Thus, LTE values for this element, computed with stellar atmosphere parameters corrected by overionization effects should give correct abundances. The lithium abundance was estimated for all stars included in our sample by fitting synthetic spectra

Table 4. LTE abundances with respect to the Sun.

Ident	A228	A447	A575	A721	A1406	A2084	A2111	Sun
[Na/H]	−1.92		−1.91				−1.83	6.28
[Mg/H]	−2.08	−2.17	−2.21	−2.24	−2.11	−2.09	−2.15	7.53
[Ca/H]	−1.99	−2.02	−1.99	−1.98	−2.02	−1.99	−1.99	6.36
[Sc/H]	−2.00	−2.03	−1.96	−1.98	−1.92	−1.84	−2.07	2.99
[Ti/H]	−1.79	−1.69	−1.82	−1.82	−1.78	−1.68	−1.79	4.88
[Cr/H]	−2.27	−2.38	−2.36	−2.40	−2.39	−2.38	−2.35	5.61
[Fe/H]	−2.25	−2.27	−2.24	−2.23	−2.25	−2.23	−2.24	7.46
[Ni/H]	−2.22	−2.42	−2.26	−2.25	−2.31	−2.34	−2.16	6.18
[Zn/H]	−1.96	−2.00	−1.96	−1.98		−1.84	−2.21	4.60
[Ba/H]	−2.45	−2.61	−2.50	−2.51	−2.54	−2.40	−2.41	2.18

Table 5. LTE abundances with respect to the Sun (except for Li) using NLTE atmospheric parameters (e.g. $[Fe/H]_{NLTE}$ and $\log g_{NLTE}$, see text).

Ident	A228	A447	A575	A721	A1406	A2084	A2111	Sun
A(Li)	2.22	2.19	2.18	2.21	2.29	2.38	2.22	3.31
[Na1/H]	−1.88		−1.86				−1.85	6.28
[Mg1/H]	−2.13	−2.24	−2.31	−2.27	−2.15	−2.13	−2.26	7.53
[Ca1/H]	−1.92	−1.95	−1.93	−1.90	−1.93	−1.88	−1.95	6.36
[Sc2/H]	−1.81	−1.83	−1.79	−1.83	−1.75	−1.66	−1.87	2.99
[Ti1/H]	−1.72	−1.65	−1.76	−1.76	−1.71	−1.59	−1.71	4.88
[Ti2/H]	−1.60	−1.54	−1.65	−1.73	−1.66	−1.51	−1.61	4.88
[Cr1/H]	−2.39	−2.46	−2.38	−2.42	−2.34	−2.32	−2.40	5.61
[Cr2/H]	−1.97	−2.06	−2.17	−2.18			−2.03	5.61
[Fe1/H]	−2.19	−2.26	−2.20	−2.19	−2.18	−2.16	−2.19	7.46
[Fe2/H]	−2.03	−2.11	−2.06	−2.09	−2.07	−2.02	−2.05	7.46
[Ni1/H]	−2.16	−2.37	−2.20	−2.21	−2.25	−2.29	−2.09	6.18
[Zn1/H]	−1.89	−1.92	−1.88	−1.92		−1.76	−2.14	4.60
[Ba2/H]	−2.30	−2.45	−2.36	−2.38	−2.41	−2.28	−2.27	2.18

Table 6. NLTE abundances, (:) indicates resonant lines were used.

Ident	A228	A447	A575	A721	A1406	A2084	A2111
[Na/H]	−2.04	−2.50:	−2.05	−2.05:		−2.15:	−1.99
[Ca/H]	−1.82	−1.79	−1.81	−1.78	−1.80	−1.80	−1.75
[Mg/H]	−1.96	−1.99	−2.05	−2.08	−1.96	−1.94	−2.00
[Fe/H]	−2.05	−2.05	−2.03	−2.03	−2.04	−2.03	−2.01
[Na/Fe]	0.01	−0.45:	0.00	−0.02:		−0.12:	0.02
[Ca/Fe]	0.23	0.26	0.22	0.25	0.24	0.23	0.26
[Mg/Fe]	0.09	0.06	−0.02	−0.05	0.08	0.09	0.01

to the observed profiles (see, for instance, Jasniewicz et al. 1999). Secondly, gravities from Hipparcos and Fe II lines alone can be used to overcome the ionization balance difficulty (Thévenin & Idiart 1999). According to our computations, the differences between Fe II abundances derived with corrected atmospheric parameters (Table 5) and $[Fe/H]_{NLTE}$ are small. This approach was also followed by Israelian et al. (2001), who studied oxygen and iron in a sample of metal-poor subdwarfs. They concluded that gravities from Hipparcos are in good agreement with those estimated in NLTE, reducing the discrepancies between oxygen abundances derived from different lines in past studies.

3.3. NLTE abundances

Because the UV radiation field is increased in metal-poor stars, the Saha equations are not perfectly satisfied for most of the studied atoms, which are overionized. Departures from the Boltzmann equations also exist and in consequence, NLTE abundances have to be computed using the code by Carlsson (1986) and atom models for Ca, Mg and Fe according to Thévenin & Idiart (1999), Idiart & Thévenin (2000), and also for Na (Thévenin, to be published) for which accurate photoionization cross sections are available. This consists of solving for the statistical equilibrium of a multi-level atom in the stellar

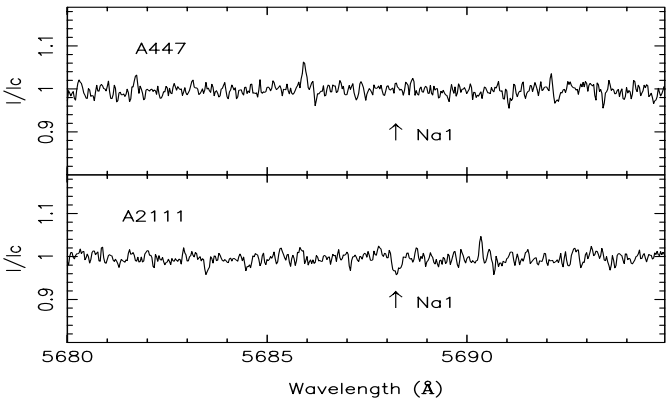

Fig. 3. Spectral region including the Na1(5688 Å) transition for A447 and A2111.

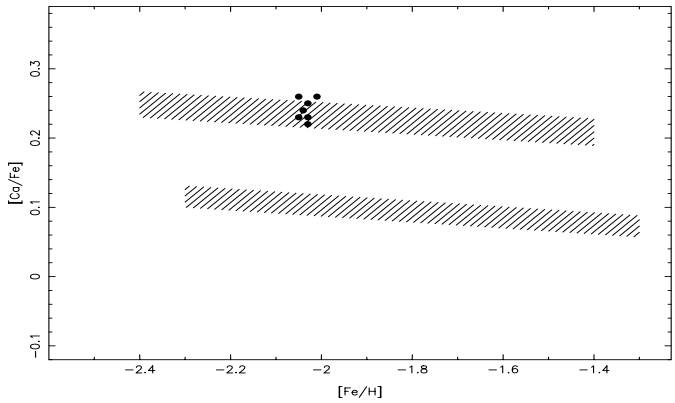

Fig. 4. [Ca/Fe] diagram, black points are NGC6397 results and the shaded zones are parallel structures from Idiart & Thévenin (2000), see Sect. 4.2, adopted error bars are ±0.1 dex for both axes.

atmosphere. A line by line comparison between the computed equivalent width and the observed one, following an iterative procedure, is performed until the desired accuracy is attained. The resulting abundances are given in Table 6. NLTE abundances of Fe were derived following Thévenin & Idiart (1999), i.e. using the curve of growth technique. $[Fe/H]_{NLTE}$ values are close to those of [FeII/H] (see Table 5), as one should expect. The NLTE abundances of Ca, Mg and Na were calculated using the following transitions: Caλ5588, Mgλ5528 and Naλ5688 and NaD. For the Mgλ5528 line, mean corrections are ≈0.12 dex, in perfect agreement with results obtained by Zhao & Gehren (2000). Note that the mean NLTE iron abundance and the mean NLTE Ca abundance give a resulting ratio $[Ca/Fe]_{NLTE}$ very similar to $[Ca/Fe]_{LTE}$ while the ratio [Mg/Fe] is slightly more affected by NLTE corrections, because NLTE corrections for Mg are significantly lower than those for Fe, which is not the case for Ca. NLTE corrections strongly depend on the nature of the atom and of the line transition studied.

It was not possible to measure the equivalent width of the Naλ5688 line for all the stars; in this case the resonant doublet was used. Na abundances derived from the resonant transition are identified with a double dot in Table 6.

4. Discussion

4.1. [Fe/H] abundances (NLTE)

Concerning the resulting [Fe/H] abundances (last column of Table 3), the first point to be emphasized is the rather small star-to-star variation. The mean NLTE iron abundance is [Fe/H] = −2.02, with a rmsd of only 0.01 dex, to be compared with our estimated error of 0.10 dex due to the uncertainties in the effective temperature and surface gravity. Such a mean value is in good agreement with the iron abundance of giants derived by Minniti et al. (1993), namely [Fe/H] = −1.94 ± 0.04, and with the results by Castilho et al. (2000), who performed a study of 16 giants and subgiants in this cluster ([Fe/H] = −2.00 ± 0.05). Five turnoff stars and three subgiants in NGC 6397 were recently studied by Gratton et al. (2000); they derived a mean iron abundance in quite agreement with our determination, but they emphasize that the ionization equilibrium is not well reproduced, with abundances from FeI lines being 0.11 dex higher than those derived from FeII lines. This is inverted with respect to our expectations we should expect, but the mean temperature adopted by those authors is about 260 K higher than the mean temperature we derived for our turnoff stars, and a similar difference is observed between the adopted mean temperature for their subgiants and those of Castilho et al. (2000).

4.2. α-elements: Ca (NLTE), Ti (LTE)

The mean abundances of calcium and titanium (magnesium will be discussed separately) from our sample are [Ca/Fe] = +0.24 ± 0.02 and [Ti/Fe] = +0.47 ± 0.06, where the former corresponds to NLTE and the latter to LTE calculations. Again we note a small star-to-star scatter. These results are also in agreement with LTE abundances derived for evolved stars by Castilho et al. (2000), who obtained [Ca/Fe] = +0.20 ± 0.07 and [Ti/Fe] = +0.43 ± 0.12.

According to the results of Idiart & Thévenin (2000), the data points in the plots [Ca/Fe] or [Mg/Fe] against [Fe/H] for field dwarfs show a "lumpy" distribution, which appears, particularly in the case of calcium, when NLTE effects are taken into account. The $[Ca/Fe]_{NETL}$ ratios of our program stars match quite well one of those structures, represented as shaded zones in Figs. 4 and 5. The reason(s) for the appearance of these structures is (are) still unknown.

4.3. Iron group (LTE): Sc, Cr, Ni

Abundances of Sc, Cr and Ni were all derived from LTE calculations. Their mean values derived from Table 4 are [Sc/Fe] = +0.27 ± 0.07, [Cr/Fe] = −0.12 ± 0.05, [Ni/Fe] = −0.03 ± 0.08. These abundances are entirely compatible with those derived for field stars of same metallicity (McWilliam et al. 1995; Ryan et al. 1996).

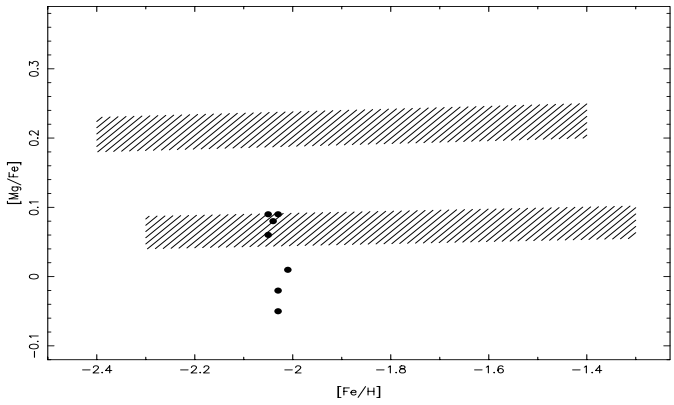

Fig. 5. [Mg/Fe] diagram, same as Fig. 4.

4.4. n-capture element: Ba (LTE)

The only n-capture element studied is barium because of the lack of measurable lines for other n-elements. For field stars, the [Ba/Fe] ratio increases from values around −1.5 at [Fe/H] ≈ −3.5 up to near-solar values at metallicities around [Fe/H] ≈ −1.6, and then remains more or less constant. Thus, NGC 6397 is in a "transition region". The mean LTE abundance derived from data in Table 4 is [Ba/Fe] = -0.24 ± 0.06. This value is compatible with the mean abundance derived from the sample of evolved stars by Castilho et al. (2000), namely, [Ba/Fe] = -0.16 ± 0.12 and is in remarkable good agreement with abundances of field stars having comparable metallicity (McWilliam et al. 1995; Ryan et al. 1996).

4.5. Zinc (LTE)

Few results exist on the abundance of Zn in metal poor stars, leaving incomplete the understanding of the nucleosynthetic origin of this element. The present status on the Zn abundance in halo stars was reviewed by Sneden et al. (1991), who showed that in the metallicity range $-2.5 <$ [Fe/H] < -1.5 the relative Zn abundance is $-0.20 <$ [Zn/Fe] < 0.25 dex. Our LTE results (Table 4) give a mean value [Zn/Fe] = +0.25 dex. It is worth mentioning that Sneden et al. (1991) used 7.60 dex (see their Tables 3 and 4) for the solar iron abundance, instead of 7.46 adopted in the present work. An additional correction of −0.02 dex should be applied for Zn due to same reason and there is a difference of −0.03 between the adopted log gf. Therefore, in order to compare the results by Sneden et al. (1991) with our mean value, one should shift the former by ∼0.1 dex. Under these conditions, our results are in good agreement with those authors.

Zinc is an interesting element also because its interstellar lines have been detected in absorption spectra of quasars (damped Lyman-alpha systems). Moreover, zinc can be considered as a fair and useful indicator of the gas phase metallicity of interlopers, since it is expected to be far less depleted in dust grains than iron.

The [Zn/H] vs. redshift correlation was recently reviewed by Savaglio (2000), who derived the relation

$$[\mathrm{Zn/H}] = -0.32z - 0.40. \quad (3)$$

If one assumes that the gas seen in absorption is associated with the early "halo-phase" of the interlopers and that the outer galactic halo evolved chemically in a similar way, then from the above equation and our derived Zn abundance, one obtains an equivalent redshift $z \approx 4.75$. This redshift corresponds to an age given by the equation

$$t_{\mathrm{age}}(z) = \frac{1}{H_0} \int_0^z \frac{\mathrm{d}x}{(1+x)[\Omega_{\mathrm{v}} + \Omega_{\mathrm{m}}(1+x)^3]^{1/2}} \quad (4)$$

where H_0 is the Hubble parameter and we assumed a "flat" world model such as $\Omega_{\mathrm{m}} + \Omega_{\mathrm{v}} = 1$, where Ω_{m} is the density parameter including both baryonic and dark matter, and Ω_{v} is the density parameter of the vacuum energy density. Assuming $H_0 = 65\ \mathrm{km\,s^{-1}Mpc^{-1}}$, $\Omega_{\mathrm{m}} = 0.25$ and $\Omega_{\mathrm{v}} = 0.75$, satisfying of the constraints imposed by primordial nucleosynthesis, type Ia supernovae, Boomerang and Maxima-I data, one obtains $t = 14$ Gyr for the presumed age of the cluster. This result must be taken with a grain of salt since the zinc abundance vs. redshift relationship above is questionable and will probably not be applicable to the inner metal-rich clusters. These objects have a higher mean rotational velocity, a smaller velocity dispersion (Zinn 1985; Borges & de Freitas Pacheco 1988), and were formed in regions with a higher star formation rate.

4.6. Magnesium (NLTE)

The mean NLTE abundance of magnesium, derived from Table 6 is [Mg/Fe] = $+0.04 \pm 0.06$. The NLTE analysis performed by Idiart & Thévenin (2000) for 252 dwarfs and subgiants indicates a large scatter in the diagram [Mg/Fe] vs. [Fe/H] with some lumpy structures. Our sample stars are located in the lower envelope of the diagram by Idiart & Thévenin (see Fig. 5), with four stars on one of those structures. Similar abundances were derived by Gratton et al. (2000), who obtained a mean abundance ratio [Mg/Fe] = $+0.08 \pm 0.03$ from five dwarfs in NGC 6397. Such an agreement remains true even if their abundances are corrected to our temperature scale.

The chemical enrichment of the halo depends on the type II supernovae rate and on the time-scale required for the ejecta to be completely mixed with the interstellar gas. Thus, it is reasonable to imagine that the halo was chemically inhomogeneous before total mixing occurs, and that stars formed during this early phase may have intrinsic abundance differences at the same metallicity. Model calculations by Argast et al. (2000) (see also Travaglio et al. 1999) suggest that the halo is unmixed if [Fe/H] < -3.0 and only when [Fe/H] > -2.0 is the halo gas well mixed, with the abundance pattern reflecting the yields integrated over the initial mass function. In the metallicity range $-3.0 <$ [Fe/H] < -2.0 there is a transition region

from the unmixed to the well-mixed interstellar medium. Field stars can be found in all these phases, but metal-poor globular clusters were mainly formed during the transition period whereas metal-rich ones were formed when the gas was already well mixed. The large scatter found in the diagram [Mg/Fe] vs. [Fe/H] by Idiart & Thévenin (2000) is consistent with the stochastic scenario developed by Argast et al. (2000).

4.7. Sodium (NLTE)

The analysis of the sodium abundance in NGC 6397 is more complex. The mean abundance ratio excluding the star A447 is almost solar, namely [Na/Fe] $= -0.02 \pm 0.06$. The star A447 seems to be sodium-deficient. Figure 3 shows the spectral region including the transition Naλ5688 for A447 and A2111. The line is clearly seen in the latter but not in the former and this behaviour can be translated into abundance differences, since both stars have similar atmospheric parameters. Note that the Naλ5688 line is difficult to measure even for the star A2111, and the Naλ5682 line is undetectable in all spectra because its log gf is 0.3 lower when compared to that of the line Naλ5688. In consequence, this line could not be extracted from our data since its equivalent width is always less than 3–4 mÅ. The de-blending of the NaD lines also suggests a sodium deficiency in A447, since the equivalent width measured for this star is almost one half of that obtained for the other objects. This is confirmed because NaD lines also have about one half the equivalent widths of other stars. Gratton et al. (2000) have also derived Na abundances for five dwarfs in NGC 6397. Three stars have almost solar values whereas the other two dwarfs are overabundant. Using our temperature scale, the mean sodium abundance from their data is [Na/Fe] $= +0.04 \pm 0.11$, a value consistent with our results. Concerning Na abundances in evolved stars, Minniti et al. (1996) studied five giants in this cluster. Their data indicate a mean value essentially solar but with star-to-star variations. Minniti et al. (1996) concluded that their data are consistent with the Na vs. O anti-correlation. However, if the giants studied by Castilho et al. (2000) as well as those by Gratton et al. (2000) are included in a plot, one obtains essentially a scatter diagram, supporting Na abundance variations among evolved stars.

4.8. Lithium (LTE)

Lithium is of particular interest since it is of primordial origin and easily depleted in stellar interiors.

It is important to note that lithium should not have been affected by dilution in the program stars; they have an effective temperature higher than the one needed to start the first dredge-up (this happens around 5700 K in a stellar model typical of our NGC 6397 sample; see e.g. Charbonnel et al. 2000). The mean Li abundance of our sample, in a scale where $\varepsilon(\mathrm{Li}) = \log\,[n(\mathrm{Li})/n(\mathrm{H})] + 12$,

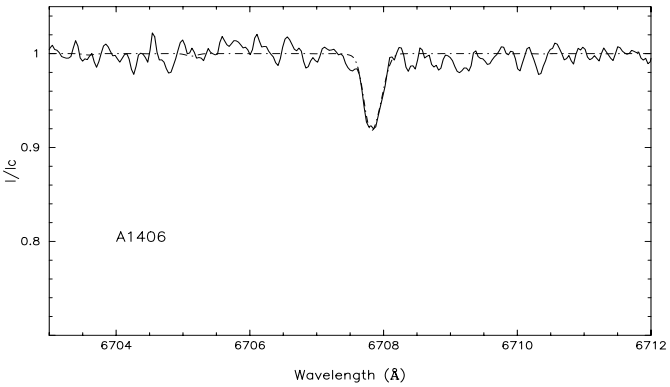

Fig. 6. Fit of the lithium blend for the star A1406.

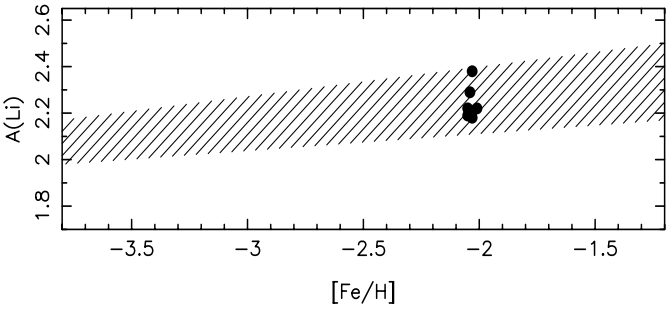

Fig. 7. Derived Li abundances of the program stars (filled dots) compared with the diagram by Ryan et al. (2001) (shaded band). Error bars are ±0.1 dex for both axes.

is equal to $\varepsilon(\mathrm{Li}) = 2.23 \pm 0.07$. Again, we emphasize the small scatter among the stars. Our results agree with the study by Pasquini & Molaro (1996) on three turnoff stars of NGC 6397 which are located in the same temperature range. They are also consistent with the general trend of lithium abundance in metal-poor stars (see Fig. 7). However, a larger dispersion of ε(Li) was found in subgiant stars of M 92 by Boesgaard et al. (1998), who favor differential depletion due to different rotation histories to explain their data. It is worth noticing that the M 92 subgiants show other peculiar abundances, in particular under and overabundances of Mg and Al respectively (see Sect. 1) which could be due to intra-cluster pollution. More data for lithium are needed in globular cluster dwarfs. This is of particular importance if one wants to combine Li data of cluster and halo stars to constrain the primordial abundance of this element and its evolution in the early Galaxy.

5. Conclusions

We derived chemical abundances for several elements in seven turnoff stars in NGC 6397. The cluster metallicity is [Fe/H] $= -2.02 \pm 0.01$ and no significant star-to-star abundance variations were detected, indicating that NGC 6397 is a homogeneous cluster. Moreover, the iron abundance derived from turnoff stars are in good agreement with abundances derived from subgiants (Castilho et al. 2000) as expected.

Calcium and titanium have abundances in agreement with those derived for giants and subgiants in this cluster, while the abundances of the iron peak elements agree with those of field stars with similar iron content. These abundances are consistent with the predictions of the stochastic model by Argast et al. (2000), when the expected abundance ratio dispersion at a given metallicity is taken into account, in spite of the uncertainties still present in the supernova yields. We note that our [Ca/Fe] and [Mg/Fe] ratios match onto the lumpy structures found in the plots by Idiart & Thévenin (2000), when halo dwarfs are considered. More data on clusters with different metallicities are certainly required for a better understanding of these structures.

Magnesium is almost solar and small variations among the stars were found within the expected errors, but a definitive conclusion must wait for a larger sample. In agreement with Gratton et al. (2000), no Mg vs. Na anticorrelation seems to be present in our turnoff stars, although an intriguing enhancement of the magnesium abundance in subgiants, with respect to dwarfs, is suggested from the data of these authors, again concerning only a few objects.

When data from different authors are considered (Minniti et al. 1996; Castilho et al. 2000; Gratton et al. 2000), they suggest that sodium variations are clearly present in evolved stars. The mean Na abundance ratio in dwarfs is almost solar, but there is some evidence of intriguing star-to-star variations. A447 is deficient by almost a factor of three with respect to the other stars and this trend is also verified in dwarfs studied by Gratton et al. (2000). Similar Na variations in turnoff stars were also detected in 47 Tuc and in NGC 6752 (Cottrel & Da Costa 1981; Briley et al. 1994, 1995; Gratton et al. 2000), which are difficult to understand in either the framework of the primordial or deep-mixing scenarios. The reality of these variations must be confirmed by other studies and by analyses adopting the same procedure, atmospheric models, and physical parameters to derive NLTE chemical abundances.

Acknowledgements. We thank the UVES team for building an excellent spectrograph and the ESO staff at Paranal Observatory for the service observations. We are grateful to the referee for his comments, which improved the presentation of this paper and also to B. Gladman for other improvement of the manuscript. We thank INSU and PNPS for financial supports. Part of this work has been performed using the computing facilities provided by the program "Simulations Interactives et Visualisation en Astronomie et Mécanique (SIVAM)" at the observatoire de la Côte d'Azur.

References

Alcaino, G., Liller, W., Alvarado, F., et al. 1997, AJ, 114, 1067
Alonso, A., Arribas, S., & Martínez-Roger, C. 1996, A&A, 313, 873
Argast, D., Samland, M., Gerhard, O. E., & Thielemann, F. K. 2000, A&A, 356, 873
Asplund, M., Gustafsson, B., Kiselman, D., & Eriksson, K. 1997, A&A, 318, 521
Axer, M., Fuhrmann, K., & Gehren, T. 1995, A&A, 300, 751
Ballester, P., Modigliani, A., Boitquin, O., et al. 2000, The Messenger, 101, 31
Boesgaard, A. M., Deliyannis, C. P., Stephens, A., & King, J. R. 1998, ApJ, 493, 206
Borges, A. C. A., & de Freitas Pacheco, J. A. 1989, ApSS, 153, 67
Briley, M. M., Hesser, J. E., Bell, R. A., Bolte, M., & Smith, G. H. 1994, AJ, 108, 2183
Briley, M., Smith, V., Suntzeff, N., et al. 1995, Nature, 383, 604
Carlsson, M. 1986, Thesis, Uppsala Astronomical Observatory Report, 33
Carlsson, M., Rutten, R. J., Bruls, J. H. M. J., & Schukina, N. G. 1994, A&A, 288, 860
Castilho, B. V., Pasquini, L., Allen, D. M., Barbuy, B., & Molaro, P. 2000, A&A, 361, 92
Cavallo, R. M., Sweigart, A. V., & Bell, R. A. 1998, ApJ, 492, 575
Cayrel, R. 1987, IAU Symp., 132, 345
Cayrel, R., & Traving, G. 1960, ZA, 50, 239
Charbonnel, C., Brown, J. A., & Wallerstein, G. 1998, A&A, 332, 204
Charbonnel, C., Deliyannis, C. P., & Pinsonneault, M. H. 2000, IAU Symp., 198, 87
Cohen, J. G. 1975, ApJ, 197, 117
Cottrell, P. L., & Da Costa, G. S. 1981, ApJ, 245, 79
da Costa, G. S. 1998, IAU, 189, 193
Dekker, H., D'Odorico, S., Kaufer, A., Delabre, B., & Kotzlowski, H. 2000, Proc. Conf. SPIE, 4008-61
Denissenkov, P. A., & Denisenkova, S. N. 1990, Sov. Ast. Lett., 16, 275
Denissenkov, P. A., & Weiss, A. 1996, A&A, 308, 773
Denissenkov, P. A., Da Costa, G. S., Norris, J. E., & Weiss, A. 1998, A&A, 333, 926
Djorgovski, S. G. 1993, sdgc. Proc, 373
Edvardsson, B., Andersen, J., Gustafsson, B., et al. 1993, A&A, 275, 101
Eggen, O. 1960, MNRAS of South Africa, 19, 115
Gratton, R. G., Bonifacio, P., Bragaglia, A., et al. 2001, A&A, 369, 87
Gustafsson, B., Bell, R., Ericksson, K., & Nordlund, Å. 1975, A&A, 57, 235
Harris, W. E. 1996, AJ, 112, 1487
Holweger, H. 1979, Les éléments dans l'Univers, Proc. 22nd Liège Intern. Astrophys. Colloqium, Université de Liège, 11
Idiart, T., & Thévenin, F. 2000, ApJ, 541, 207
Israelian, G., Rebolo, R., Garcia Lopez, R., et al. 2001, ApJ, 551, 833
Ivans, I., Sneden, C., Kraft, R. P., et al. 1999, AJ, 118, 1273
Jasniewicz, G., Parthasarathy, M., de Laverny, P., & Thévenin, F. 1999, A&A, 342, 831
King, J. R., Stephens, A., & Boesgaard, A. M. 1998, AJ, 115, 666
Kraft, R. P., Sneden, C., Langer, G. E., & Prosser, C. F. 1992, AJ, 104, 645
Kraft, R. P., Sneden, C., Langer, G. E., & Shetrone, M. D. 1993, AJ, 106, 1490
Kraft, R. P. 1994, PASP, 106, 553
Kraft, R. P., Sneden, C., Langer, G. E., Shetrone, M. D., & Bolte, M. 1995, AJ, 109, 2586

Kraft, R. P., Sneden, C., Smith, G. H., et al. 1997, AJ, 113, 279
Kraft, R. P., Sneden, C., Smith, G. H., Shetrone, M. D., & Fulbright, J. 1998, AJ, 115, 1500
Langer, G. E., Hoffman, R., & Sneden, C. 1993, PASP, 105, 301
Magain, P. 1988, IAUS, 132, 485
Martin, G. A., Fuhr, J. R., & Wiese, W. L. 1988, J. Phys. Chem. Ref. Data, 17, Suppl. 3
McWilliam, A., Preston, G. W., Sneden, C., & Searle, L. 1995, AJ, 109, 2757
Miles, B. M., & Wiese, W. L. 1969, NBS Techn. Note, 474
Minniti, D., Geisler, D., Peterson, R. C., & Claria, J. J. 1993, ApJ, 413, 548
Minniti, D., Peterson, R. C., Geisler, D., & Claria, J. J. 1996, ApJ, 470, 953
Norris, J. E., & da Costa, G. S. 1995, ApJ, 447, 680
Palacios, A., Leroy, F., Charbonnel, C., & Forestini, M. 2000, ghgc. conf., 67
Paltoglou, G., & Norris, J. E. 1989, ApJ, 336, 185
Pasquini, L., & Molaro, P. 1996, A&A, 307, 761
Peterson, R. C. 1980, ApJ, 237, 87
Pilachowski, C. A., Sneden, C., Kraft, R. P., & Langer, G. E. 1996, AJ, 112, 545
Plez, B., Brett, J. M., & Nordlund, A. 1992, A&A, 256, 551
Ryan, S. G., Norris, J. E., & Beers, T. C. 1996, ApJ, 471, 254
Ryan, S. G., Kajino, T., Beers, T. C., et al. 2001, ApJ, 548
Savaglio, S. 2000, IAUS, 204, 24
Sekiguchi, M., & Fukugita, M. 2000, AJ, 120, 1072
Shetrone, M. D. 1996a, fogh. conf., 383
Shetrone, M. D. 1996b, AJ, 112, 2639
Smith, G., & Raggett, D. J. 1981, J. Phys. B, 14, 4015-24
Sneden, C., Gratton, R. G., & Crocker, D. A. 1991, A&A, 246, 354
Sneden, C. 1999, Ast. Spa. Sci, 265:1-4 (Kluwer Academic Publishers, Dordrecht), 145
Sneden, C., Kraft, R. P., Prosser, C. F., & Langer, G. E. 1992, AJ, 104, 2121
Sneden, C., Kraft, R. P., Shetrone, M. D., et al. 1997, AJ, 114, 1964
Stehlé, C., Mazure, A., Feautrier, N., & Nollez, G. 1983, A&A, 127, 263
Thévenin, F. 1989, A&AS, 77, 137
Thévenin, F. 1990, A&AS, 82, 179
Thévenin, F., & Idiart, T. 1999, ApJ, 521, 753
Travaglio, C., Galli, D., Gallino, R., et al. 1999, ApJ, 521, 691
Vauclair, S., & Charbonnel, C. 1998, ApJ, 502, 372
Vidal, C. R., Cooper, J., & Smith, E. W. 1973, ApJS, 214, 25
Warner, B. 1968, MNRAS, 140, 53
Weiss, A., Denissenkov, P. A., & Charbonnel, C. 2000, A&A, 356, 181
Wiese, W. L., Smith, M. W., & Miles, B. M. 1969, NSRDS-NBS 22
Wiese, W. L., & Martin, G. A. 1980, NSRD-NBS, 68, Part II
Zhao, G., & Gehren, T. 2000, A&A, 362, 1077
Zinn, R. 1985, ApJ, 293, 424
Zucker, D., Wallerstein, G., & Brown, J. A. 1996, PASP, 108, 911